Supplementary Information for

Graph-structured gravity model enhances transferable pedestrian flow prediction

Fatemeh Nourmohammadi[1], **Taha H. Rashidi**[1], **Meead Saberi**[1]

[1]Research Center for Integrated Transport Innovation, School of Civil and Environmental Engineering, University of New South Wales, Sydney, 2052, Australia

Correspondence to: meead.saberi@unsw.edu.au

1 Data Summary

Supplementary Table 1 presents descriptive statistics for all input variables used in model development and evaluation across the four study cities: Melbourne, Brisbane, Seattle, and Chicago. The variables include socio-demographic characteristics, built environment attributes, land-use composition, and network topology measures, computed separately for origins and destinations.

Land-use composition (e.g., percentage of commercial, educational, industrial, parkland, transport, and water areas) and the number of points of interest (POIs) are important for the attraction terms in gravity-based models. Network topology metrics—such as node degree, closeness, betweenness, PageRank, and core number—were computed using the pedestrian network graphs extracted from OpenStreetMap. These metrics capture structural differences between the four urban networks, which play a central role in TL-GNet's ability to learn transferable patterns.

The heterogeneity in population size, POI density, and network measures across cities highlights the importance of robust model architectures that can accommodate diverse urban forms and data distributions. This variability also provides a challenging testbed for evaluating model transferability across different spatial, socio-economic, and infrastructural contexts.

Supplementary Table 1. Descriptive statistics of input variables across cities

City	Melbourne					Brisbane					Seattle					Chicago				
Variables	count	mean	std	min	max	count	mean	std	min	max	count	mean	std	min	max	count	mean	std	min	max
Weighted walking trips	6794	149.499	44.547	82.760	489.380	3468	132.572	66.668	21.856	713.640	354	228.89	497.52	1.39	4806.76	1165	274.322	268.659	62.260	1720.170
Hop	6794	1.229	0.672	0.000	2.000	3468	1.076	0.684	0.000	2.000	354	0.737	0.631	0	2	1165	0.852	0.672	0	2
Population origin	6794	476.720	246.929	0.000	4355.000	3468	432.080	187.492	0.000	1889.000	354	4437.695	1106.789	1187	8420	1165	4003.484	1681.140	980	11373
Population destination	6794	470.399	256.096	0.000	4355.000	3468	435.465	187.276	0.000	1889.000	354	4461.754	1159.601	1187	8420	1165	3989.979	1667.618	980	11373
Number of stations destination	6794	3.200	3.575	0.000	83.000	3468	5.503	6.403	0.000	70.000	354	17.588	14.573	0	106	1165	17.941	19.397	0	192
Number of Links/Number of Nodes destination	6794	0.423	0.075	0.302	1.500	3468	0.449	0.067	0.333	1.000	354	3.012	0.310	2.190	3.552	1165	3.362	0.278	2.384	3.910
Intersection count destination	6794	88.069	128.889	0.000	2842.000	3468	66.092	97.857	1.000	2181.000	354	905.946	645.029	99	5371	1165	424.686	362.923	11	3724
% of commercial landuse destination	6794	11.428	22.734	0.000	100.000	3468	7.108	17.482	0.000	100.000	354	44.798	40.766	0	100	1165	13.519	10.648	0	68.261
% of education landuse destination	6794	4.135	11.116	0.000	100.000	3468	5.775	14.885	0.000	100.000	354	0.239	1.725	0	24.557	1165	5.189	8.210	0	56.688
% of industrial landuse destination	6794	2.412	12.189	0.000	100.000	3468	1.916	9.677	0.000	100.000	354	4.951	14.261	0	79.360	1165	2.865	7.099	0	67.507
% of parkland landuse destination	6794	9.773	19.412	0.000	100.000	3468	11.906	19.834	0.000	100.000	354	0.575	2.849	0	35.207	1165	7.489	14.586	0	90.202
% of transport landuse destination	6794	0.905	5.242	0.000	100.000	3468	0.664	4.655	0.000	71.219	354	20.900	27.595	0	100	1165	4.823	7.425	0	47.926
% of water landuse destination	6794	0.074	1.469	0.000	54.795	3468	0.743	5.370	0.000	72.700	354	4.702	15.179	0	97.453	1165	0.430	2.104	0	18.024
Number of stations origin	6794	2.987	3.397	0.000	83.000	3468	5.454	5.890	0.000	50.000	354	16.859	13.654	0	106	1165	18.214	17.891	0	143
Number of Links/Number of Nodes origin	6794	0.424	0.079	0.294	1.500	3468	0.449	0.066	0.333	1.000	354	3.010	0.307	2.190	3.552	1165	3.363	0.276	2.384	3.910
Intersection Count origin	6794	85.276	122.461	1.000	2842.000	3468	65.999	96.932	1.000	2181.000	354	890.056	646.321	99	5371	1165	432.185	355.485	31	3724
% of commercial landuse origin	6794	10.981	22.721	0.000	100.000	3468	6.954	17.309	0.000	100.000	354	44.650	39.481	0	100	1165	13.598	10.316	0	55.558
% of education landuse origin	6794	4.618	11.637	0.000	100.000	3468	6.118	15.315	0.000	100.000	354	0.226	1.348	0	9.872	1165	5.647	9.094	0	56.688
% of industrial landuse origin	6794	2.303	11.800	0.000	100.000	3468	1.956	9.871	0.000	100.000	354	5.296	14.552	0	79.360	1165	2.863	7.099	0	57.972
% of parkland landuse origin	6794	9.351	18.497	0.000	100.000	3468	11.790	19.802	0.000	100.000	354	0.547	2.802	0	35.207	1165	7.840	15.195	0	90.202
% of transport landuse origin	6794	0.572	3.679	0.000	100.000	3468	0.712	5.124	0.000	71.219	354	20.621	26.307	0	100	1165	4.864	7.659	0	47.926
% of water landuse origin	6794	0.074	1.466	0.000	54.795	3468	0.731	5.357	0.000	72.700	354	4.964	15.438	0	97.453	1165	0.375	1.905	0	16.771
Household median age origin	6794	37.887	9.274	0.000	83.000	3468	39.725	11.256	0.000	85.000	354	42.375	12.190	8	80	1165	36.363	9.016	7	69
Weekly household income origin	6794	1621.676	605.838	0.000	4749.000	3468	1775.540	737.444	0.000	8000.000	354	2238.840	1045.020	96.154	4807.692	1165	1768.702	870.726	144.231	3846.154
Traveled distance	6794	550.682	295.864	10.000	5200.000	3468	630.512	433.307	10.000	3980.000	354	1060.656	789.059	103.000	5788.288	1165	729.413	669.715	0	8638.937
Node degree origin	6794	32.246	11.555	0.000	113.000	3468	25.707	8.374	0.000	64.000	354	10.992	5.888	0	31	1165	23.530	12.191	0	46
Closeness origin	6794	0.014	0.006	0.000	0.021	3468	0.003	0.002	0.000	0.007	354	0.018	0.012	0	0.049	1165	0.028	0.016	0	0.048
Betweenness origin	6794	0.002	0.004	0.000	0.040	3468	0.000	0.000	0.000	0.005	354	0.000	0.001	0	0.003	1165	0.001	0.001	0	0.011
Pagerank origin	6794	0.000	0.000	0.000	0.000	3468	0.000	0.000	0.000	0.000	354	0.004	0.003	0.002	0.012	1165	0.001	0.001	0.000	0.002
Core origin	6794	13.566	4.392	0.000	26.000	3468	9.543	2.923	0.000	16.000	354	6.282	3.536	0	14	1165	11.922	6.036	0	18
Node degree destination	6794	31.016	12.966	0.000	113.000	3468	24.366	9.486	0.000	64.000	354	9.477	6.138	0	31	1165	21.918	12.923	0	46
Closeness destination	6794	0.014	0.006	0.000	0.021	3468	0.003	0.002	0.000	0.007	354	0.019	0.011	0	0.049	1165	0.028	0.016	0	0.047841
Betweenness destination	6794	0.001	0.004	0.000	0.040	3468	0.000	0.000	0.000	0.005	354	0.000	0.001	0	0.003	1165	0.001	0.001	0	0.009
Pagerank destination	6794	0.000	0.000	0.000	0.000	3468	0.000	0.000	0.000	0.000	354	0.004	0.003	0.002	0.012	1165	0.001	0.001	0.000	0.002
Core destination	6794	13.330	4.542	0.000	26.000	3468	9.322	3.048	0.000	16.000	354	5.969	3.698	0	14	1165	11.578	6.151	0	18

2 Impact of Attraction Specification on Model Performance

Supplementary Table 2 compares two alternative specifications of the destination attraction term in the gravity model across the four cities including a POI-based formulation ("POIs") and a land-use composition formulation ("Land mix"). Performance is reported using CPC, RMSE, NRMSE, Pearson correlation, and JSD. Results show modest differences between the two variants. In the Australian cases, Land mix yields slightly higher CPC and lower RMSE than POIs (e.g., Brisbane: CPC 0.10 vs. 0.09; RMSE 50.38 vs. 52.01) and notably improves JSD in Brisbane (0.832 vs. 0.848), while Melbourne exhibits a small CPC/RMSE gain but a near-tie in correlation and a marginally higher JSD. In the U.S. cases, the two specifications perform nearly identically on CPC; POIs have a marginal edge on RMSE and JSD (e.g., Chicago: RMSE 172.58 vs. 173.03; JSD 0.670 vs. 0.673), whereas correlation differences remain small and near zero in both cities. Overall, enriching attraction with land-use mix modestly benefits the Australian settings, while POI counts perform on par (and occasionally slightly better on error/divergence) in Seattle and Chicago.

Supplementary Table 2. Comparison of gravity model performance across different attraction term formulations. Each variant is evaluated using CPC, RMSE, correlation, and JSD to assess predictive accuracy in modeling pedestrian flows.

	Model	CPC	RMSE	NRMSE	Corr.	JSD
Melbourne, Australia	POIs	0.09	51.079	3.623	0.005	0.830
	Land mix	0.10	50.842	3.606	0.005	0.831
Brisbane, Australia	POIs	0.09	52.010	3.831	-0.004	0.848
	Land mix	0.10	50.381	3.710	-0.001	0.832
Seattle, USA	POIs	0.21	253.035	3.948	0.019	0.640
	Land mix	0.21	253.971	3.962	0.001	0.650
Chicago, USA	POIs	0.20	172.584	2.927	-0.018	0.670
	Land mix	0.20	173.029	2.934	-0.015	0.673

3 SHAP Values

SHAP values are used to interpret the contribution of each input feature to the model's predictions. By attributing changes in the output to individual features based on cooperative game theory, SHAP provides a consistent measure of feature importance. In our analysis, SHAP values highlight the relative influence of graph-topological variables, distance, and attraction terms on predicted pedestrian flows, offering insights into the model's decision-making process beyond aggregate performance metrics.

Supplementary Figure 1. Distribution of SHAP values for all features in TL-GNet for Melbourne (a), Brisbane (b), Seattle (c), and Chicago (d). Features are shown on the vertical axis, sorted from most to least influential. Each point represents an origin–destination pair, with blue indicating low feature values and red indicating high values. Points are jittered vertically to improve visibility of overlaps. The horizontal position shows the SHAP value for that pair, indicating whether the feature increases or decreases the predicted pedestrian flow probability. For example, large distances tend to deter travel, while shorter distances are associated with higher predicted commuter flows.

4 Model Transferability Across Cities

To further assess the robustness and transferability of our approach, we present a series of comparative analyses. Supplementary Figure **2** reports the performance of TL-GNet against the baseline Deep Gravity (DG) model across all city-to-city transfer scenarios, evaluated using four complementary metrics: Correct Prediction Count (CPC), Root Mean Squared Error (RMSE), Jensen–Shannon Divergence (JSD), and correlation (Corr.). Supplementary Figure **3** extends this evaluation by summarizing results across all transfer cases, providing boxplot comparisons and percentage improvements that highlight the consistent advantages of TL-GNet over DG. Finally, Supplementary Figure **4** presents a sensitivity analysis with respect to the regularization parameter λ, demonstrating that TL-GNet maintains stable and reliable performance across a wide range of hyperparameter settings.

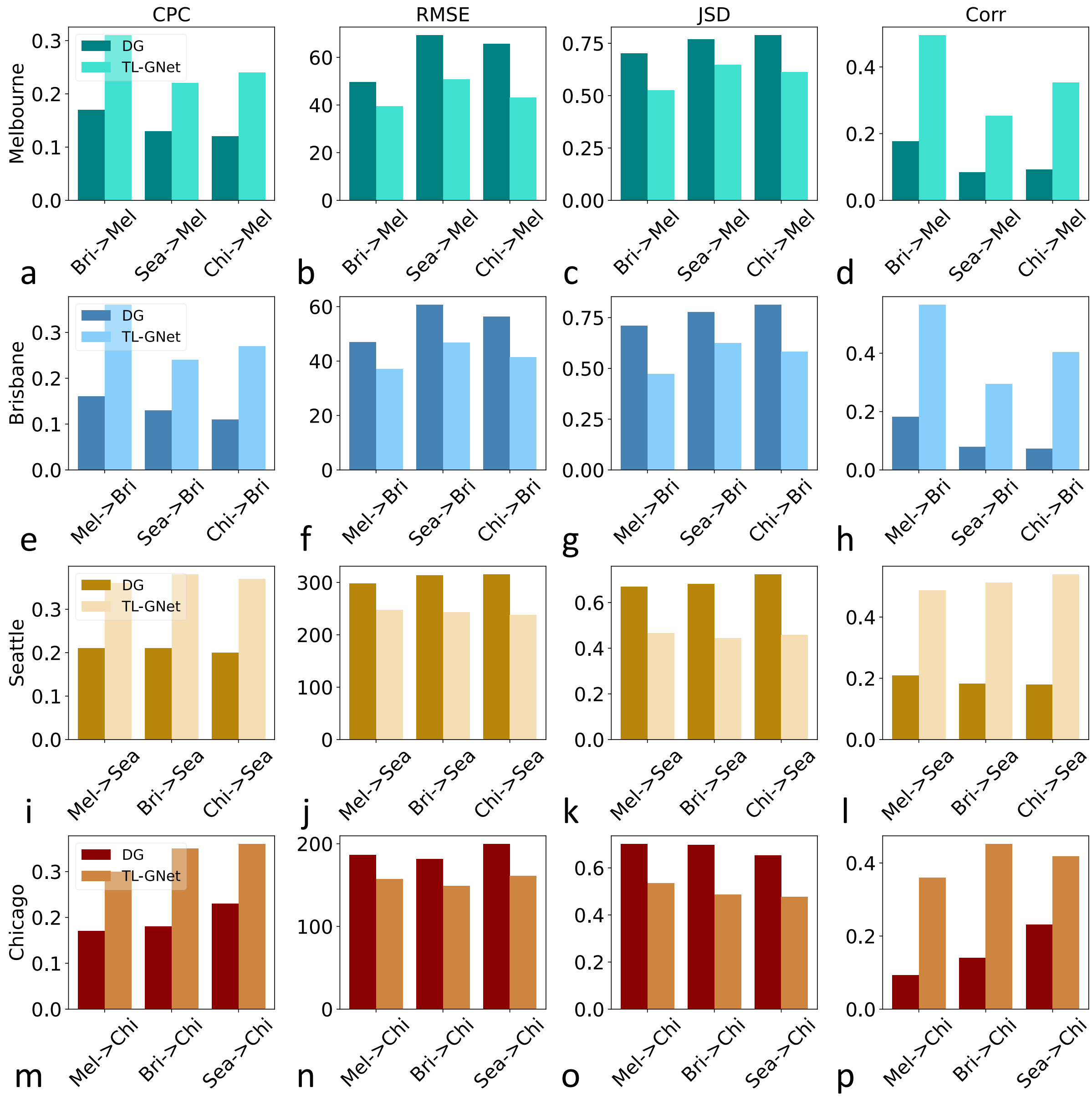

Supplementary Figure 2. Comparison of Deep Gravity (DG) and our Transferable Laplacian Regularization GravityNet (TL-GNet) models across four key performance metrics—Correct Prediction Count (CPC), Root Mean Squared Error (RMSE), Jensen-Shannon Divergence (JSD), and Correlation (Corr.)—for all city-to-city transfer scenarios. Each row represents a target city (Melbourne, Brisbane, Seattle, and Chicago), while each column corresponds to a different performance metric. The bars show the performance of each model when transferred from the remaining three cities. Subplots (a) to (p) provide a breakdown of results by target city and metric.

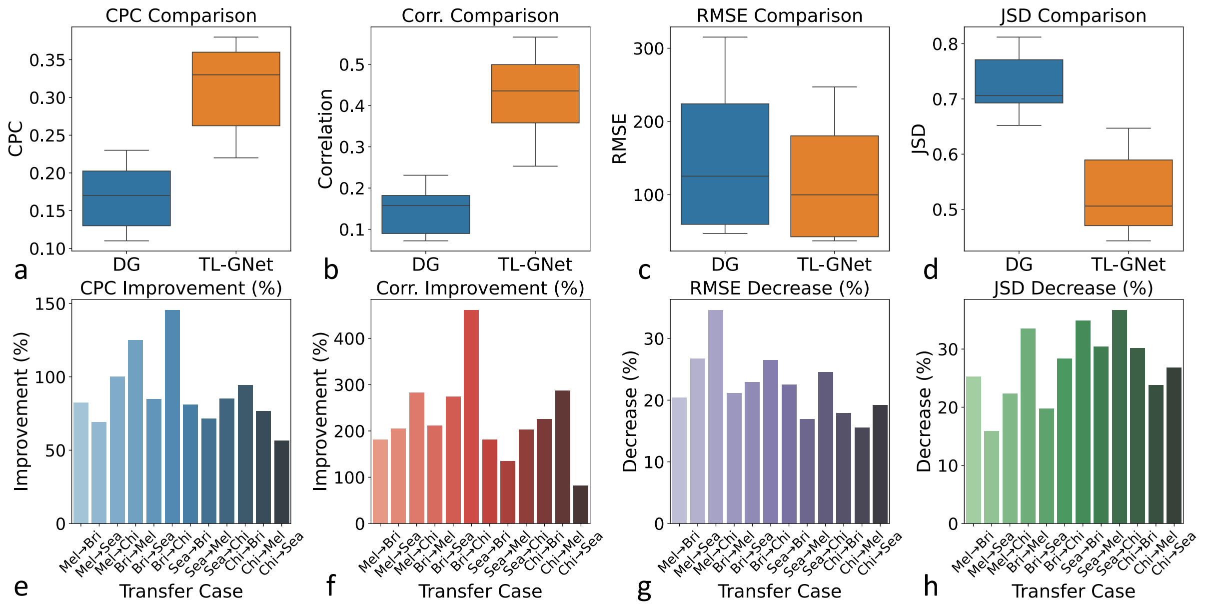

Supplementary Figure 3. Performance comparison between the Deep Gravity (DG) model and the Transferable Laplacian Regularization GravityNet (TL-GNet) model across city-to-city transfer cases. Subplots (a) and (b) present boxplots comparing CPC and correlation values, respectively, for both models across all scenarios. Subplots (c) and (d) compare RMSE and JSD, showing that TL-GNet yields lower error and divergence values. Subplots (e) to (h) illustrate the percentage improvement or reduction for each transfer case.

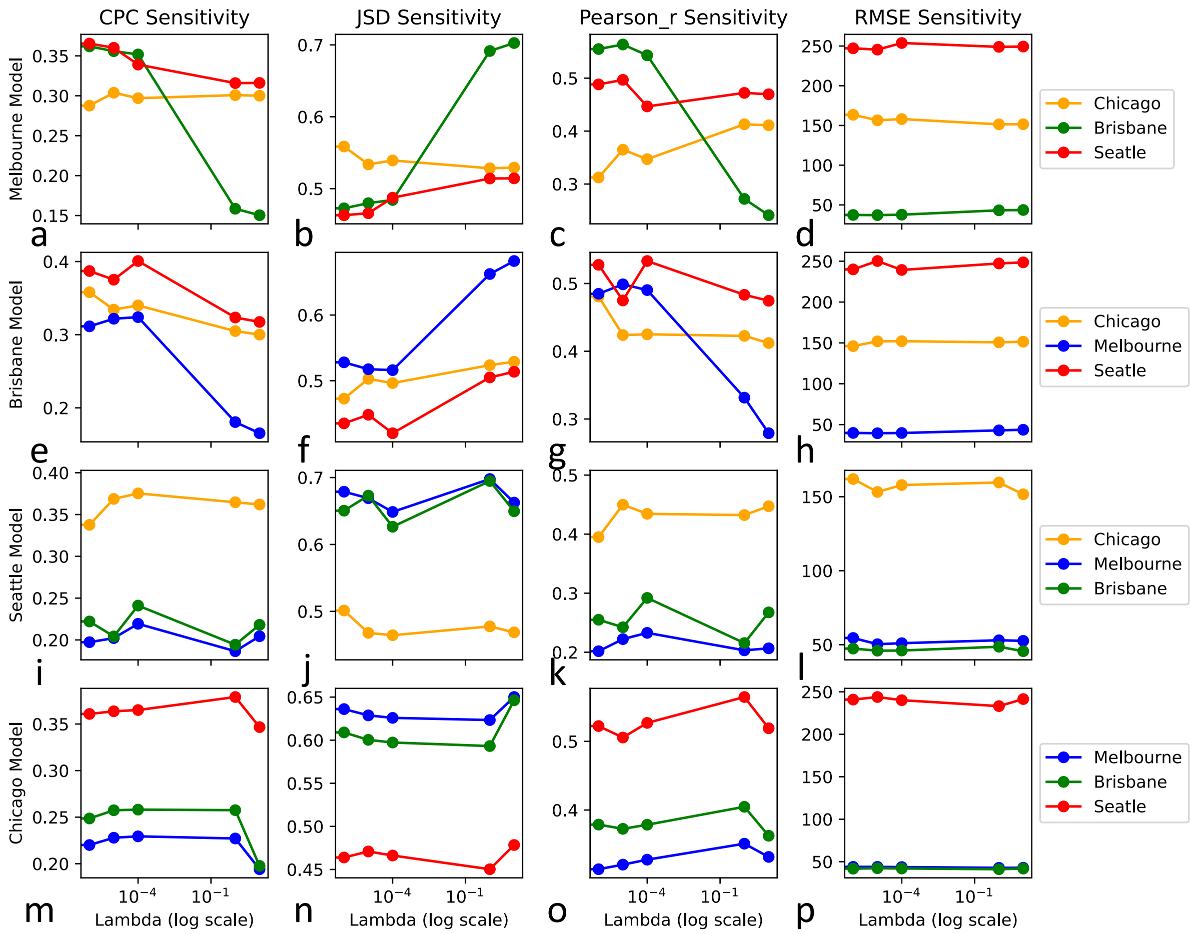

Supplementary Figure 4. Sensitivity analysis of the Transferable Laplacian Regularization GravityNet (TL-GNet) model with respect to the regularization parameter λ (log scale). The analysis examines how variations in λ affect model performance across four metrics: Correct Prediction Count (CPC), Jensen–Shannon Divergence (JSD), Pearson correlation coefficient, and Root Mean Squared Error (RMSE). Each row corresponds to a model trained on data from one of the four cities (Melbourne, Brisbane, Seattle, Chicago), and each subplot shows the model's performance on the other three cities. Subplots (a–d), (e–h), (i–l), and (m–p) correspond to models trained on Melbourne, Brisbane, Seattle, and Chicago, respectively.

5 Definitions, Metrics and Formulations

We employ several network centrality and structural measures computed using Python's NetworkX package. This section outlines the key definitions and formulations applied in our analysis.

5.1 Hop Count

The hop count is the number of edges in the shortest path between two nodes, u and v. It represents the minimum number of steps required to travel from one node to another in the network. This measure is particularly useful for assessing accessibility and connectivity in unweighted graphs.

$$\text{HopCount}(u, v) = \text{length of shortest path from } u \text{ to } v \tag{1}$$

5.2 PageRank

PageRank is a centrality measure that quantifies the importance of a node based on the structure of incoming links. The underlying assumption is that a node is important if it is referenced by other important nodes. Originally developed by Google to rank web pages, PageRank is widely used to identify influential nodes in a network. It incorporates a damping factor (commonly set to 0.85) to model the probability of continuing a random walk on the graph [Wang, 2004, Li et al., 2023]. The PageRank of node i is defined as:

$$PR(i) = \frac{1-d}{N} + d \sum_{j \in \mathcal{N}(i)} \frac{PR(j)}{k_j^{\text{out}}} \tag{2}$$

where d is the damping factor, N is the total number of nodes, $\mathcal{N}(i)$ is the set of nodes linking to i, and k_j^{out} is the out-degree of node j.

5.3 Core Number

The core number of a node is the largest integer k for which the node belongs to a k-core. A k-core is a maximal subgraph in which every node has degree at least k. The core number captures how deeply embedded a node is within the network and is often used to identify cohesive subgroups [Hell and Nešetřil, 1992].

$$c(v) = \max\{k \mid v \in \text{the } k\text{-core of } G\} \tag{3}$$

5.4 Node Degree

The degree of a node v is the number of direct connections it has to other nodes. In an undirected graph, this corresponds to the count of all incident edges. Node degree provides a basic measure of connectivity and indicates a node's influence within its immediate neighborhood.

$$\deg(v) = |\{u \in V \mid (u, v) \in E\}| \tag{4}$$

5.5 Betweenness Centrality

Betweenness centrality quantifies the extent to which a node lies on the shortest paths between pairs of other nodes. It reflects a node's potential to mediate communication or flow within the network. Nodes with high betweenness centrality often act as bottlenecks or key connectors[White and Borgatti, 1994].

$$C_B(v) = \sum_{s \neq v \neq t} \frac{\sigma_{st}(v)}{\sigma_{st}} \tag{5}$$

where σ_{st} is the total number of shortest paths from s to t, and $\sigma_{st}(v)$ is the number of those paths that pass through node v.

5.6 Closeness Centrality

Closeness centrality measures how close a node is to all other nodes in the network. It is defined as the inverse of the average shortest path distance from the node to every other node. Nodes with high closeness centrality can reach others more quickly and efficiently, making them effective at spreading information [Evans and Chen, 2022, Freeman, 1977].

$$C_C(v) = \frac{1}{\sum_{u \in V \setminus \{v\}} d(u, v)} \tag{6}$$

5.7 Pearson Correlation Coefficient

The Pearson correlation coefficient quantifies the strength and direction of the linear relationship between two variables (e.g., sets of flows). It is defined as:

$$r = \frac{\sum_{i=1}^{n}(y_i - \bar{y})(\hat{y}_i - \bar{\hat{y}})}{\sqrt{\sum_{i=1}^{n}(y_i - \bar{y})^2} \cdot \sqrt{\sum_{i=1}^{n}(\hat{y}_i - \bar{\hat{y}})^2}} \tag{7}$$

where n is the sample size (number of flows), y_i is the actual (observed) flow, $\hat{y}_i$ is the predicted (generated) flow, $\bar{y}$ is the mean of the observed flows, $\bar{\hat{y}}$ is the mean of the predicted flows.

5.8 Root Mean Squared Error (RMSE)

The Root Mean Squared Error (RMSE) measures the standard deviation of prediction errors (residuals). It is defined as:

$$\text{RMSE} = \sqrt{\frac{1}{n}\sum_{i=1}^{n}(y_i - \hat{y}_i)^2} \tag{8}$$

It penalizes larger errors more than smaller ones, making it sensitive to outliers. Lower RMSE values indicate better prediction accuracy.

5.9 Jensen-Shannon Divergence (JSD)

The Jensen–Shannon Divergence (JSD) measures the similarity between two probability distributions. Unlike the Kullback–Leibler Divergence (KLD), it is symmetric and bounded within $[0, 1]$. Given two distributions P and Q, and their average $M = \frac{1}{2}(P + Q)$, the JSD is defined as:

$$M = \frac{1}{2}(P + Q)$$

the JS divergence is defined as:

$$\text{JSD}(P\|Q) = \frac{1}{2}\text{KLD}(P\|M) + \frac{1}{2}\text{KLD}(Q\|M) \tag{9}$$

The KLD quantifies how one probability distribution diverges from another reference distribution. For discrete distributions P and Q over the same space X, it is defined as:

$$\text{KLD}(P\|Q) = \sum_{x \in X} P(x) \log\left(\frac{P(x)}{Q(x)}\right) \tag{10}$$

KLD is always non-negative and asymmetric, i.e., $\text{KLD}(P\|Q) \neq \text{KLD}(Q\|P)$. It equals 0 if and only if $P = Q$.

References

[Evans and Chen, 2022] Evans, T. S. and Chen, B. (2022). Linking the network centrality measures closeness and degree. *Communications Physics*, 5(1):172.

[Freeman, 1977] Freeman, L. C. (1977). A set of measures of centrality based on betweenness. *Sociometry*, pages 35–41.

[Hell and Nešetřil, 1992] Hell, P. and Nešetřil, J. (1992). The core of a graph. *Discrete Mathematics*, 109(1-3):117–126.

[Li et al., 2023] Li, Z., Fu, D., and He, J. (2023). Everything evolves in personalized pagerank. In *Proceedings of the ACM Web Conference 2023*, pages 3342–3352.

[Wang, 2004] Wang, Z. (2004). Improved link-based algorithms for ranking web pages. In *International Conference on Web-Age Information Management*, pages 291–302. Springer.

[White and Borgatti, 1994] White, D. R. and Borgatti, S. P. (1994). Betweenness centrality measures for directed graphs. *Social networks*, 16(4):335–346.